

Theoretical investigation of carbon defects and diffusion in α -quartz

Christof Köhler,^{1,4} Zoltán Hajnal,^{1,2} Péter Deák,³ Thomas Frauenheim,¹ and Sándor Suhai⁴

¹*Theoretische Physik, FB6, Universität-GH Paderborn, Warburger Str. 100, D-33095 Paderborn, Germany*

²*Research Institute for Technical Physics and Materials Science, P.O.B. 49, H-1525 Budapest, Hungary*

³*Department of Atomic Physics, Budapest University of Technology and Economics, Budafoki út 8, H-1111 Budapest, Hungary*

⁴*German Cancer Research Center, Department of Molecular Biophysics, Im Neuenheimer Feld 230, D-69120 Heidelberg, Germany*

(Received 11 April 2001; published 8 August 2001)

The geometries, formation energies, and diffusion barriers of carbon point defects in silica (α -quartz) have been calculated using a charge-self-consistent density-functional based nonorthogonal tight-binding method. It is found that bonded interstitial carbon configurations have significantly lower formation energies (on the order of 5 eV) than substitutionals. The activation energy of atomic C diffusion via trapping and detrapping in interstitial positions is about 2.7 eV. Extraction of a CO molecule requires an activation energy < 3.1 eV but the CO molecule can diffuse with an activation energy < 0.4 eV. Retrapping in oxygen vacancies is hindered—unlike for O₂—by a barrier of about 2 eV.

DOI: 10.1103/PhysRevB.64.085333

PACS number(s): 66.30.Jt, 73.20.-r, 81.65.Mq

I. INTRODUCTION

Defects in SiO₂ have received much attention over the last decades because of the outstanding importance of this material as an insulating layer in microelectronic devices. Research has been focused mainly on the properties of the native defects as well as of the dopants used in Si device technology. Comparatively little is known, however, about other impurities, e.g. carbon, in SiO₂.

With the advent of SiC-based devices, for which SiO₂ is also the native oxide, the behavior of carbon inside SiO₂ became a major issue. SiC/SiO₂ interface-state concentrations are orders of magnitude above those of Si/SiO₂,¹ and carrier traps inside the oxide layer¹ generally degrade device performance. Furthermore, there are signs of interface features unknown for Si, related to incomplete removal of carbon. Spectroscopic studies¹ suggest the presence of C nanoclusters at the SiC/SiO₂ interface, giving rise to defect states resembling defects in amorphous hydrogenated carbon, *a*-C:H. In recent experiments² it has been shown that excess oxygen is needed to extract carbon atoms of such layers, and the resulting C-O species diffuses fast in high-quality SiO₂.

There are also experimental indications³ that during oxidation of SiC the outdiffusion of carbonaceous species is a fast process. The oxidation rate has been thought to be limited by the indiffusion of oxygen.³ Experimental estimates for the activation energy of oxygen diffusion in vitreous silica range from 4.7 eV (Ref. 4) for an atomic lattice diffusion mechanism to 1.17 eV (Ref. 5) for the molecular diffusion. Theoretical works in ideal crystalline SiO₂ lead to lower barrier heights than observed in experiment due to the lack of the traps represented by the Si dangling bonds of real vitreous silica. Hamann⁶ calculated the diffusion barrier for a particular SiO₂ lattice defect involving interstitial atomic oxygen, the peroxy defect, to be 1.3 eV, whereas Chelikowsky *et al.*⁷ just recently proposed a saddle point for molecular oxygen diffusion with a barrier height of 0.7 eV. Since the strength of a single Si-O bond is about 4.7 eV, the experimentally observed barrier for atomic O diffusion is probably related to dangling bond traps. Apart from that both

experiment and theory predict a relatively fast O diffusion in high-quality SiO₂. Therefore, the formation of the fast diffusing carbonaceous species from bonded carbon atoms has to be discussed as the crucial step in hindering the oxidation via slower, eventually incomplete, removal of carbon.

There are additional experiments which indicate that carbon nanoclusters may also form inside a SiO₂ layer. The use of organosilanes (TEOS) in Si device technology causes the formation of a carbon-rich phase in SiO₂.⁸ The fast diffusion of carbonaceous species is confirmed in this experiment, too.⁸ Infrared (IR) spectra obtained from a similar experiment⁹ show the presence of C=O double bonds in the SiO₂ layer. The IR peak intensity of this defect gradually increases with decreasing quality of the SiO₂ layer. That also points to the trapping of C in an imperfect SiO₂ network. No carbon aggregation in the oxide was found in Ref. 2 where the SiO₂ layer had a very low dangling bond density to begin with.

While diffusion of oxygen in SiO₂ itself has been thoroughly examined experimentally^{5,4,10} as well as theoretically,^{6,7,11,12} we are not aware of such detailed experimental or theoretical studies on the diffusion of carbon in SiO₂. In this work therefore we focus on the basic carbon-related defects and their diffusion mechanisms in SiO₂. We first explore possible defect configurations of atomic carbon in an otherwise perfect SiO₂ lattice and then calculate barriers for diffusion paths, which may lead to removal of the carbon impurity from the lattice.

II. COMPUTATIONAL APPROACH

For the atomistic simulation of carbon defects in SiO₂ we used the self-consistent-charge density-functional-based tight-binding (SCC-DFTB) method.^{13,14} The predecessor¹⁵ of the SCC-DFTB approach has already been successfully applied to SiO₂ systems.¹⁶ For the calculations presented herein we have constructed new basis sets for the calculation of the TB matrix elements and the repulsive pair potential. These have also been tested and provide reasonable results for de-

TABLE I. Total energies of molecules and solids used in the calculation of defect formation energies.

C atom in graphite	-47.21 eV
Si atom in Si bulk	-35.29 eV
O ₂ molecule	-178.14 eV
CO molecule	-137.58 eV
CO ₂ molecule	-229.12 eV

fects in SiC (Refs. 17 and 18) and for oxygen on SiC surfaces.¹⁹

We use crystalline α -quartz (SiO₂) as a model substance because its topology and short-range order²⁰ are similar to amorphous SiO₂. The optimized geometry (experimental values²¹ in parentheses) of the hexagonal unit cell is $a = 2.49$ Å (2.46 Å) and $c = 5.43$ Å (5.41 Å) with a Si-O bond length of 1.62 Å (1.60 Å) and a SiOSi-angle of 143.5° (144.6°). For calculating the formation energy of defects, supercells with 243 atoms were used. This size was sufficient to guarantee convergence of the formation energies with respect to variations of the number of atoms and the cell volume; the change in formation energy induced by increasing the number of atoms from 162 to 243 is less than 0.02 eV. Smaller supercells with 108 and 162 atoms were then used for the calculation of diffusion barriers to economize on computer time. The Γ -point approximation for the electronic band structure energy was found to be sufficiently accurate for all sizes. The gap size in our calculations is 9.6 eV which is in reasonable agreement with the reported experimental value of 8.9 eV,²² while *ab initio* data for the band gap are about 5.59 eV (Refs. 23–25) in recent works. Although our method is DFT based, the tight-binding formalism may compensate the well-known underestimation of semiconductor band gaps by DFT. We note, however, that this is not a systematic correction and do not generally claim good predictions of the band gap.

Formation energies were calculated with respect to the ideal SiO₂ crystal, graphitic carbon, molecular oxygen, and crystalline silicon:

$$E_{\text{formation}} = E_{\text{SiO}_2 \text{ crystal}}^{\text{with defect}} - E_{\text{SiO}_2 \text{ crystal}}^{\text{ideal}} - E_{\text{carbon atom}} + E_{\text{oxygen molecule}} + E_{\text{silicon crystal}}.$$

The last two terms are only added if the concentration of the two species, silicon and oxygen, changes in the supercell containing the defect with respect to the ideal SiO₂ stoichiometry, i.e., for substitutional defects. The energy of the carbon atom is either the energy of one atom in graphite or the

TABLE II. Formation energies of some oxygen lattice point defects in SiO₂.

	SCC-DFTB	Pacchioni and Ierano ^a
Peroxyl defect	1.2 eV	1.7 eV
Oxygen vacancy	6.1 eV	6.1 eV
Frenkel defect	7.0 eV	7.6 eV

^aReferences 28 and 30.

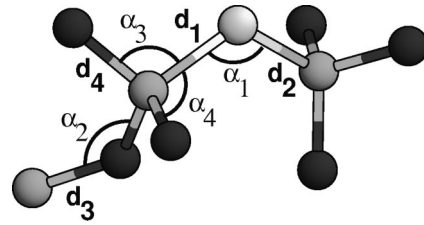


FIG. 1. Carbon on oxygen site, C_O. Only the vicinity of the defect is shown. Oxygen, dark; silicon, light; carbon, white. $d_1 = 1.86$ Å, $d_2 = 1.86$ Å, $d_3 = 1.63$ Å, $d_4 = 1.63$ Å, $\alpha_1 = 117^\circ$, $\alpha_2 = 137^\circ$, $\alpha_3 = 103^\circ$, $\alpha_4 = 109^\circ$.

energy in a CO or CO₂ molecule obtained by subtracting the appropriate O₂ total energy from the energy of the carbonaceous species. All defect formation energies rise by 3.77 eV if the energy of the carbon atom in CO₂ is used instead of the energy in graphite. The total energies of the molecules and the atoms in the elemental solids used in this calculation are summarized in Table I.

To find the saddle point configurations the algorithm of Kaukonen *et al.*²⁶ which is based on a reaction coordinate approach, and the ART algorithm of Barkema and Mousseau²⁷ were used.

To validate our investigations we have calculated formation energies for some oxygen lattice defects in SiO₂ previously studied by Pacchioni and Ierano.²⁸ The results are summarized in Table II. Pacchioni and Ierano²⁸ carried out Hartree-Fock calculations with second-order Møller-Plesset perturbation for a correlation correction on small clusters involving hydrogen atoms with fixed positions to saturate dangling bonds. Despite the very different methods and system sizes the results are in reasonable agreement. The lower formation energies in the 243-atom DFTB supercell calculation are mainly due to the higher relaxational freedom.

The diffusion of oxygen in α -quartz through neighboring peroxy configurations has been calculated by Hamann⁶ using a small 27-atom supercell (with three inequivalent \vec{k} points) in a first-principles DFT generalized gradient approximation (GGA) calculation. The formation energies (with respect to the O₂ molecule³⁰) of the peroxy defect and of the saddle point configuration along the diffusion path

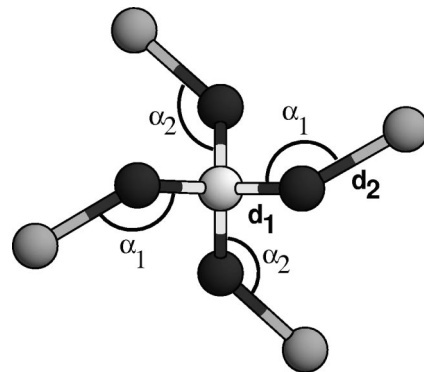


FIG. 2. Carbon on silicon site, C_{Si}. Only the vicinity of the defect is shown. Oxygen, dark; silicon, light; carbon, white. $d_1 = 1.42$ Å, $d_2 = 1.65$ Å, $\alpha_1 = 132^\circ$, $\alpha_2 = 137^\circ$.

TABLE III. Formation energies of carbon defects in SiO₂ with respect to O₂, graphite, and silicon bulk.

C _O	10.0 eV
C _{Si}	11.9 eV
CO _O	5.6 eV
Carboxyl	4.8 eV
C _i	7.7 eV
CO _i +V _O	5.9 eV

were found to be 1.6 eV and 2.9 eV, respectively (cf. Table II). Using the same supercell and a $2 \times 2 \times 3$ MP (Ref. 29) set of \mathbf{k} vectors in a SCC-DFTB calculation, we obtain 1.4 eV and 3.2 eV, respectively. The difference in the energy of the saddle point configuration is typical between the two methods. The 162-atom unit cell ($k=0$ approximation) gave 1.2 eV and 3.0 eV, respectively. The bond lengths of the saddle point configuration here are still within 3% of the values given by Hamann.

III. GEOMETRIES AND FORMATION ENERGIES OF CARBON DEFECTS

Amid the various possible carbon defects we first considered the two substitutionals, carbon on an oxygen site, C_O, and on a silicon site, C_{Si}. The geometries of the energetically minimized structures are shown in Figs. 1 and 2, respectively. While the C-Si bond lengths for C_O, 1.86 Å, are in the range known from SiC (1.89 Å in 4H-SiC) in the case of C_{Si} full relaxation to the usual C-O bond lengths which could be expected for a single bond is prevented by the surrounding lattice, resulting in a bond with a C-O distance of 1.42 Å. The formation energies of these two defects are the highest of all studied defects (see Table III), making them unlikely to occur in experimentally detectable concentrations in SiO₂.

The other defects involve an interstitial carbon atom in an otherwise stoichiometric SiO₂ lattice. The geometry of the unbonded interstitial carbon atom, C_i, is shown in Fig. 3. The distance to the nearest-neighbor oxygen atom is 1.83 Å; the distance to the nearest-neighbor silicon atom is 2.42 Å.

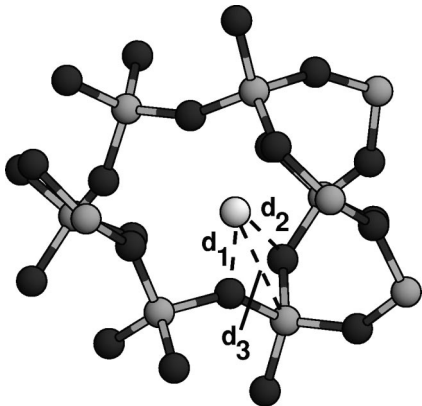


FIG. 3. Interstitial carbon atom, C_i. Only the vicinity of the defect is shown. Oxygen, dark; silicon, light; carbon, white. $d_1 = 1.83$ Å, $d_2 = 1.95$ Å, $d_3 = 2.42$ Å.

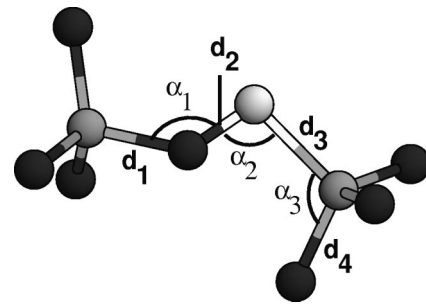


FIG. 4. Carbon and oxygen on oxygen site, CO_O. Only the vicinity of the defect is shown. Oxygen, dark; silicon, light; carbon white. $d_1 = 1.67$ Å, $d_2 = 1.30$ Å, $d_3 = 1.89$ Å, $d_4 = 1.64$ Å, $\alpha_1 = 128^\circ$, $\alpha_2 = 125^\circ$, $\alpha_3 = 110^\circ$.

The formation energy of 7.7 eV is the highest of the interstitial carbon defects.

The chemically bonded form of the carbon interstitial has two metastable configurations. The first configuration (split interstitial), denoted CO_O (see Fig. 4), is similar in geometry to the peroxy defect. The carbon and the oxygen atoms share a regular oxygen lattice site. The C-O bond length of 1.30 Å compared to 1.17 Å in the CO₂ molecule indicates a single bond; the Si-O (1.64 Å) and Si-C (1.89 Å) bond lengths are in the range known from SiO₂ (1.62 Å) and SiC, respectively. The other configuration is the carboxyl defect, as depicted in Fig. 5. Here the carbon atom is on the oxygen site, bonded to the two silicon neighbors, while the oxygen atom is bonded to the carbon atom. The C-O bond length of 1.23 Å, compared to 1.17 Å in CO₂, indicates a double bond whereas the Si-C-Si angle of 130° is typical for close to *sp*²-like hybridization of the carbon atom. This configuration could be the initial configuration for the removal of carbon if atomic oxygen attacks a Si-C-Si bond at the SiC/SiO₂ interface, provided oxygen is available, e.g., from atomic diffusion which involves the peroxy defect.

The carboxyl and the CO_O defects, shown in Figs. 5 and 4, have the lowest formation energies, 4.8 eV and 5.6 eV, respectively (Table III). Especially in the carboxyl configuration the coordination and the chemical bonding of the atoms are ideal. Experimentally detectable concentrations of these defects could be present in SiO₂ layers, especially at the SiC/SiO₂ interface.

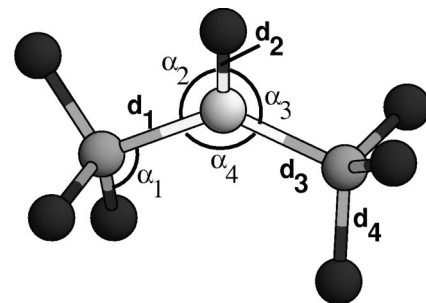


FIG. 5. Carboxyl defect. Only the vicinity of the defect is shown. Oxygen, dark; silicon, light; carbon, white. $d_1 = 1.87$ Å, $d_2 = 1.23$ Å, $d_3 = 1.88$ Å, $d_4 = 1.62$ Å, $\alpha_1 = 110^\circ$, $\alpha_2 = 114^\circ$, $\alpha_3 = 115^\circ$, $\alpha_4 = 130^\circ$.

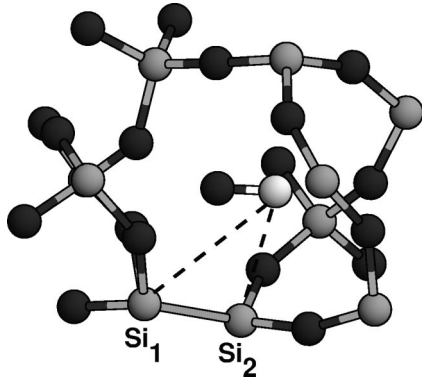


FIG. 6. CO molecule adjacent to oxygen vacancy, $\text{CO}_i + \text{V}_O$. Only the vicinity of the defect is shown. Oxygen, dark; silicon, light; carbon, white. C-O distance 1.1 Å, Si-Si distance 2.33 Å, $\text{Si}_1\text{-C} = 3.39$ Å, $\text{Si}_2\text{-C} = 2.7$ Å.

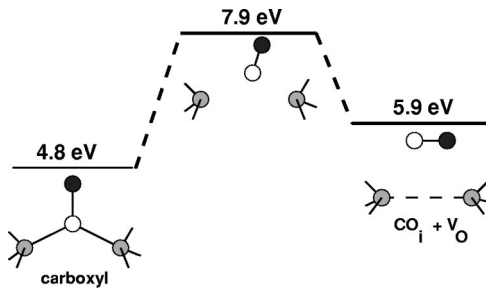


FIG. 7. Schematics of the activation step of the molecular diffusion starting from the carboxyl configuration, Fig. 5, and ending in the $\text{CO}_i + \text{V}_O$ configuration, Fig. 6. The saddle point geometry is depicted in Fig. 9. The formation energies of the local minima are given along with the energy of the saddle point in the same scale. Oxygen, dark; silicon, light; carbon, white.

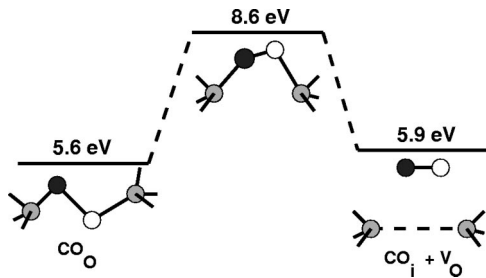


FIG. 8. Schematics of the activation step of the molecular diffusion starting from the CO_O configuration, Fig. 4, and ending in the $\text{CO}_i + \text{V}_O$ configuration, Fig. 6. The saddle point geometry could not be stabilized. The formation energies of the local minima are given along with the energy of the saddlepoint in the same scale. Oxygen, dark; silicon, light; carbon, white.

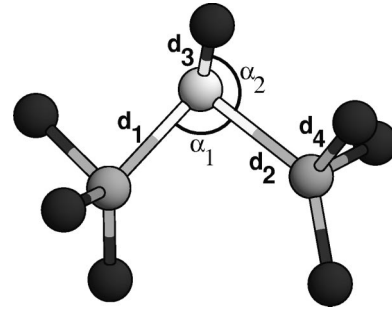


FIG. 9. Saddle point configuration between the carboxyl defect and $\text{CO}_i + \text{V}_O$. Only the vicinity of the defect is shown. Oxygen, dark; silicon, light; carbon, white. $d_1 = 1.99$ Å, $d_2 = 2.17$ Å, $d_3 = 1.21$ Å, $d_4 = 1.64$ Å, $\alpha_1 = 90^\circ$, $\alpha_2 = 96^\circ$.

The last defect we calculated is a CO molecule adjacent to an oxygen vacancy, $\text{CO}_i + \text{V}_O$. This configuration could also be involved in the removal of built-in carbon from the SiO_2 lattice. The geometry is shown in Fig. 6. The Si-Si distance of 2.33 Å is close to that in the oxygen vacancy in pure α -quartz, which is 2.32 Å in our calculations and 2.43 Å according to Pacchioni and Ierano.²⁸

The C_i and $\text{CO}_i + \text{V}_O$ configurations, which have intermediate formation energies, could be expected to occur as transient positions in the diffusion paths for, in the case of C_i , an atomic or, in the case of $\text{CO}_i + \text{V}_O$, a molecular diffusion mechanism.

IV. BARRIER HEIGHTS FOR CARBON DEFECTS

The energetics of the defects indicate that any outdiffusion of carbon will start either from the CO_O or the carboxyl configuration which have the lowest formation energies. Based on the geometries two possible mechanisms have to be considered.

In the first, molecular, mechanism a CO molecule is pulled out from either the carboxyl configuration or the CO_O configuration, leaving an oxygen vacancy and thus giving the configuration $\text{CO}_i + \text{V}_O$. For a schematic overview see Figs. 7 and 8, respectively. The saddle point configuration for the path carboxyl \rightarrow $\text{CO}_i + \text{V}_O$ is shown in Fig. 9; the barrier height is 3.1 eV for this direction (see Table IV). The reverse process, the trapping of a CO molecule by an oxygen vacancy, has a barrier of 2.0 eV. This saddle point has one imaginary mode in the vibrational spectrum.

The other possible starting position in this first mecha-

TABLE IV. Diffusion barriers for carbon defects calculated as differences between the total energies of the minima and the saddle point configurations.

Path $a \rightarrow b$	$a \rightarrow b$	$a \leftarrow b$
Carboxyl \rightarrow $\text{CO}_i + \text{V}_O$, Fig. 7	3.1 eV	2.0 eV
$\text{CO}_O \rightarrow \text{CO}_i + \text{V}_O$, Fig. 8	3.0 eV	2.7 eV
$\text{CO}_O \rightarrow \text{C}_i$, Fig. 10	2.7 eV	0.6 eV
$\text{CO}_O \rightarrow \text{CO}_O$, Fig. 12	2.0 eV	2.0 eV
Carboxyl \rightarrow CO_O , Fig. 14	1.6 eV	0.8 eV

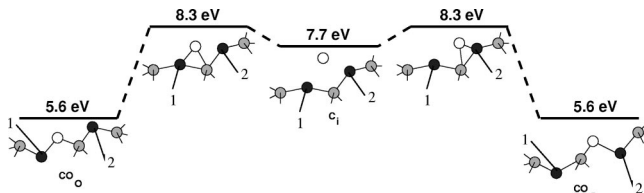


FIG. 10. Schematics of the atomic diffusion mechanism starting from the CO_O configuration, Fig. 4. The carbon atom is then in the C_i configuration, Fig. 3, before entering another CO_O configuration. The saddle point geometry is depicted in Fig. 11. The formation energies of the local minima are given along with the energy of the saddle point in the same scale. Oxygen, dark; silicon, light; carbon, white.

nism is the CO_O configuration. The saddle point between the CO_O configuration and the $\text{CO}_i + \text{V}_\text{O}$ configuration could not be stabilized because an electronic level crossing leads to a sharp decrease of total energy in the geometrical vicinity of the saddle point. However, the maximum of the total energy on this path is 3.0 eV above the energy of the CO_O configuration.

Once a CO molecule has been formed, the diffusion barriers appear to be very low. Our calculation indicates a very shallow potential energy hypersurface with a barrier < 0.4 eV for the movement of the CO molecule away from the vacancy in the c -channel direction.

The second atomic mechanism involves the CO_O and C_i configurations as local minima along the path; see Fig. 10 for an overview. The carbon atom starts from a CO_O configuration next to oxygen atom 1. It then enters through a barrier of 2.7 eV, the intermediate C_i configuration. The barrier from the C_i configuration to the next CO_O configuration is only 0.6 eV; the carbon atom is then next to oxygen atom 2. The geometry of the saddle point is shown in Fig. 11. (The barrier height for the step $\text{CO}_\text{O} \rightarrow \text{C}_i$ was estimated by moving all atoms from their initial to their final position on straight lines without any relaxation. By this we can only estimate an absolute upper limit. However, because of the defect formation energies, the lower limit for the barrier in the direction $\text{CO}_\text{O} \rightarrow \text{C}_i$, is at least 2.1 eV. We will use 2.7 eV in this paper.)

To proceed further on this path the carbon atom has to interchange position with oxygen atom 2; see Fig. 10. There are two possible paths. The first path is depicted in Fig. 12 and proceeds directly from CO_O to CO_O configuration via the

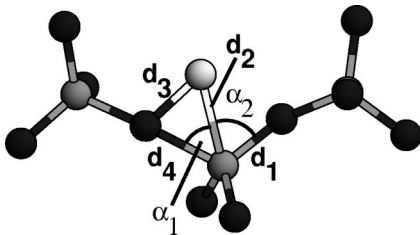


FIG. 11. Saddle point configuration between the CO_O and the C_i configuration. Only the vicinity of the defect is shown. Oxygen, dark; silicon, light; carbon, white. $d_1 = 1.62$ Å, $d_2 = 2.12$ Å, $d_3 = 1.63$ Å, $d_4 = 1.89$ Å, $\alpha_1 = 47^\circ$, $\alpha_2 = 72^\circ$.

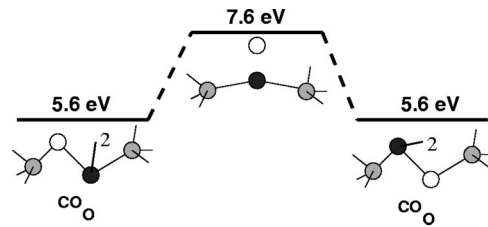


FIG. 12. Schematics of the interchange step of the atomic diffusion starting and ending in the CO_O configuration, Fig. 4. The saddle point geometry is depicted in Fig. 13. The formation energies of the local minima are given along with the energy of the saddle point in the same scale. Oxygen, dark; silicon, light; carbon, white.

saddle point configuration in Fig. 13 without the carbon occupying other local minima. The second path involves the carboxyl configuration as an intermediate local minimum; see Fig. 14 for an overview and Fig. 15 for the saddle point. The maximum barrier heights of these two interchange paths are within 2.0 eV and 1.6 eV, respectively, in the same magnitude. The highest barrier in the whole atomic diffusion mechanism is, therefore, 2.7 eV (upper limit), to be required for the activation of $\text{CO}_\text{O} \rightarrow \text{C}_i$.

The free interstitial position C_i becomes unstable in the presence of an adjacent oxygen vacancy; i.e., the carbon combines with the vacancy. Thus the diffusion of atomic carbon is likely to be disrupted if oxygen vacancies remain due to a lack of oxygen near the SiC/SiO₂ interface.

As mentioned above the interaction between an oxygen vacancy and an interstitial CO molecule is weak. This is indicated by the low barrier of < 0.4 eV for the dissociation of $\text{CO}_i + \text{V}_\text{O}$ into V_O and a separate free CO molecule and a high barrier of 2.0 eV for the trapping process $\text{CO}_i + \text{V}_\text{O} \rightarrow \text{CO}_\text{O}$ as mentioned earlier. The behavior of an oxygen molecule, initially in a configuration similar to a $\text{CO}_i + \text{V}_\text{O}$ configuration, is very different from that. There is no metastable state for the O_2 molecule in the $\text{CO}_i + \text{V}_\text{O}$ -like configuration. Instead, the oxygen molecule is trapped in the vacancy, forming a peroxy defect. These two observations—the weak interaction of the CO molecule with the vacancy opposed to the strong interaction between the vacancy and the O_2 molecule—could explain the experimental finding of

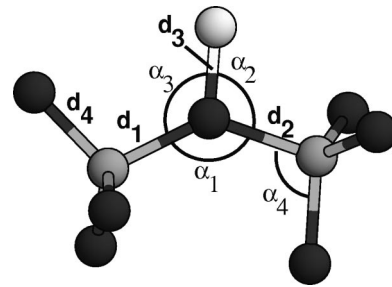


FIG. 13. Saddle point configuration between two CO_O configurations, Fig. 4, of carbon. Only the vicinity of the defect is shown. Oxygen, dark; silicon, light; carbon, white. $d_1 = 1.74$ Å, $d_2 = 1.72$ Å, $d_3 = 1.38$ Å, $d_4 = 1.60$ Å, $\alpha_1 = 134^\circ$, $\alpha_2 = 106^\circ$, $\alpha_3 = 119^\circ$, $\alpha_4 = 107^\circ$.

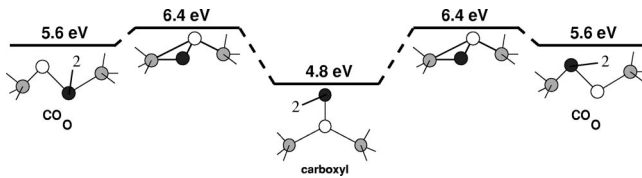


FIG. 14. Schematics of the path between the carboxyl configuration, Fig. 5, and the CO_0 configuration, Fig. 6. The saddle point geometry is depicted in Fig. 15. The formation energies of the local minima are given along with the energy of the saddle point in the same scale. Oxygen, dark; silicon, light; carbon, white.

a fast outdiffusion of carbonaceous species, once they have formed, and a slower indiffusion of oxygen in connection with the oxidation of SiC.

V. CONCLUSION

We have calculated the formation energies and diffusion barriers of carbon-related point defects in SiO_2 (α -quartz). We have found two interstitial configurations, the carboxyl defect (which has the lowest formation energy of all defects investigated) and a split interstitial with oxygen (CO_0) which have significantly lower formation energies than either substitutionals. The interstitials also represent a likely defect configuration at SiC/SiO₂ interfaces or in TEOS-grown SiO₂ layers on Si, leading to degradation of device performance in both cases. There are two possible mechanisms for the removal and outdiffusion of carbon from these interstitial positions. A CO molecule can be extracted from these defects with an activation energy of <3.1 eV. The CO molecule then diffuses without a strong coupling to the lattice with a barrier of <0.4 eV. Recapture by an oxygen vacancy is prevented by a barrier of 2 eV, unlike in the case of O₂ which is easily trapped again. Alternatively, an unbonded C_i intersti-

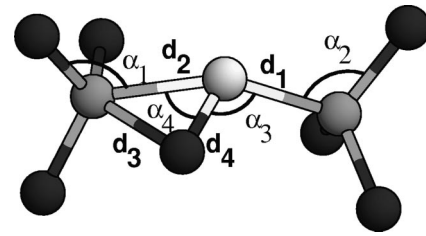


FIG. 15. Saddle point configuration between the carboxyl defect and CO_0 . Only the vicinity of the defect is shown. Oxygen, dark; silicon, light; carbon, white. $d_1=1.88$ Å, $d_2=1.98$ Å, $d_3=1.80$ Å, $d_4=1.33$ Å, $\alpha_1=104^\circ$, $\alpha_2=106^\circ$, $\alpha_3=43^\circ$, $\alpha_4=78^\circ$.

tial can be extracted from the CO_0 configuration and recaptured at the next oxygen site. The highest barrier in this diffusion process is 2.7 eV. These results show that carbon atoms can be removed from a continuous network of SiO₂ with an activation energy between 2.7 and 3.1 eV. On the other hand, CO can diffuse with a very low (0.4 eV) barrier in silica.

Our findings regarding the CO extraction and diffusion are in good qualitative agreement with the results of experiments Krafcsik *et al.*^{2,31} which indicate that carbon diffusion does not start through high-quality SiO₂ up to temperatures in excess of 900 °C,³² but then it proceeds very fast. They also show that at the temperature used for the oxidation of SiC (≈ 1200 °C), the removal of carbon from the interface should not be limited by the diffusion of C through the oxide.

ACKNOWLEDGMENTS

The authors wish to acknowledge support through DFG Grant No. Fr889/12 and the Hungarian-German bilateral Project MTA-DFG, No. 112.

- ¹V. V. Afanasev, M. Bassler, G. Pensl, and M. Schulz, *Phys. Status Solidi B* **162**, 321 (1997).
- ²O. H. Krafcsik, Gy. Vida, I. Pócsik, K. V. Josepovits, and P. Deák, *Jpn. J. Appl. Phys., Part 1* **40**, 2197 (2001).
- ³Z. Zheng, R. E. Tressler, and K. E. Spear, *J. Electrochem. Soc.* **137**, 854 (1990).
- ⁴J. Mikkelsen, Jr., *Appl. Phys. Lett.* **45**, 1187 (1984).
- ⁵F. J. Norton, *Nature (London)* **191**, 701 (1961).
- ⁶D. R. Hamann, *Phys. Rev. Lett.* **81**, 3447 (1998).
- ⁷J. R. Chelikowsky, D. J. Chadi, and N. Binggeli, *Phys. Rev. B* **62**, R2251 (2000).
- ⁸I. Mizushima, E. Kamiya, N. Arai, M. Sonoda, M. Yoshiki, S. Takagi, M. Wakamiya, S. Kambayashi, Y. Mikata, S. Mori, and M. Kashiwagi, *Jpn. J. Appl. Phys., Part 1* **36**, 1465 (1997).
- ⁹K. Sano, S. Hayashi, S. Wickramanayaka, and Y. Hatanaka, *Thin Solid Films* **282**, 397 (1996).
- ¹⁰J. D. Kalen, R. S. Boyce, and J. D. Cawley, *J. Am. Chem. Soc.* **74**, 203 (1991).
- ¹¹M. Heggie, R. Jones, C. D. Latham, S. Maynard, and P. Tole, *Philos. Mag. B* **65**, 463 (1992).

- ¹²A. Edwards and W. B. Fowler, *Phys. Rev. B* **26**, 6649 (1982).
- ¹³M. Elstner, D. Porezag, G. Jungnickel, J. Elsner, M. Haugk, Th. Frauenheim, S. Suhai, and G. Seifert, *Phys. Rev. B* **58**, 7260 (1998).
- ¹⁴Th. Frauenheim, G. Seifert, M. Elstner, Z. Hajnal, G. Jungnickel, D. Porezag, S. Suhai, and R. Scholz, *Phys. Status Solidi B* **217**, 41 (2000).
- ¹⁵D. Porezag, Th. Frauenheim, Th. Köhler, G. Seifert, and R. Kaschner, *Phys. Rev. B* **51**, 12 947 (1995).
- ¹⁶R. Kaschner, Th. Frauenheim, Th. Köhler, and G. Seifert, *J. Comput. Aided Mater. Design* **4**, 53 (1997).
- ¹⁷E. Rauls, R. Gutierrez, J. Elsner, and Th. Frauenheim, *Solid State Commun.* **111**, 459 (1999).
- ¹⁸E. Rauls, T. Lingner, Z. Hajnal, S. Greulich-Weber, Th. Frauenheim, and J.-M. Spaeth, *Phys. Status Solidi B* **217/2**, R1 (2000).
- ¹⁹E. Rauls, Z. Hajnal, P. Deák, and Th. Frauenheim, *Phys. Rev. B* (accepted).
- ²⁰R. Doremus, *J. Electrochem. Soc.* **143**, 1992 (1996).
- ²¹R. W. G. Wyckoff, *Crystal Structures* (Interscience, New York, 1963).

- ²²T. Di Stefano and D. E. Eastman, *Solid State Commun.* **9**, 2259 (1991).
- ²³Yong-nian Xu and W. Y. Ching, *Phys. Rev. B* **44**, 11 048 (1991).
- ²⁴N. Binggeli, N. Troullier, J. L. Martins, and J. R. Chelikowsky, *Phys. Rev. B* **44**, 4771 (1991).
- ²⁵Z. Fang, X. Guo, S. A. Canney, S. Utteridge, M. J. Ford, I. E. McCarthy, A. S. Kheifets, M. Vos, and E. Weigold, *Phys. Rev. B* **57**, 4349 (1998).
- ²⁶M. Kaukonen, R. M. Nieminen, P. Sitch, G. Jungnickel, D. Porezag, Th. Frauenheim, and S. Poykko, *Phys. Rev. B* **57**, 9965 (1998).
- ²⁷G. T. Barkema and N. Mousseau, *Phys. Rev. Lett.* **77**, 4358 (1996).
- ²⁸G. Pacchioni and G. Ieranò, *Phys. Rev. B* **56**, 7304 (1997).
- ²⁹H. Monkhorst and D. Pack, *Phys. Rev. B* **13**, 5188 (1976).
- ³⁰The formation energies in the table are with respect to the O₂ molecule. For the conversion from -0.7 eV with respect to atomic oxygen given in Ref. 28 half of the calculated dissociation energy of O₂, 2.4 eV, was added as suggested by the authors of Ref. 28 themselves. This 2.4 eV was also applied to the -0.86 eV formation energy of the peroxy defect calculated by Hamann. For the SCC-DFTB results half of the total energy of the O₂ molecule as calculated with SCC-DFTB including spin polarization contributions is used as reference.
- ³¹O. H. Krafcsik, K. V. Josepovits, P. Deák, L. Tóth, and B. Pécz (unpublished).
- ³²Note that in those experiments carbon comes either from an α -C:(H,O)/SiO₂ interface or from a CO gas above SiO₂.